Computers and Mathematics with Applications 62 (2011) 2601–2608

Contents lists available at SciVerse ScienceDirect

Computers and Mathematics with Applications

journal homepage: www.elsevier.com/locate/camwa

Dynamic modeling of sulfate reducing biofilms

B. D'Acunto [a,*], G. Esposito [b], L. Frunzo [a], F. Pirozzi [c]

[a] University of Naples "Federico II", Department of Mathematics and Applications, via Claudio 21, 80125, Napoli, Italy

[b] University of Cassino, Department of Mechanics, Structures and Environmental Engineering, via Di Biasio 43, 03043 Cassino (FR), Italy

[c] University of Naples "Federico II", Department of Hydraulic, Geotechnical and Environmental Engineering, via Claudio 21, 80125, Napoli, Italy

ARTICLE INFO

Article history:
Received 29 June 2011
Received in revised form 20 July 2011
Accepted 25 July 2011

Keywords:
Biofilm
Mathematical modeling
Numerical method of characteristics
Sulfate reduction
Multispecies competition in biofilm

ABSTRACT

This paper presents a mathematical model able to simulate the physical, chemical and biological processes prevailing in a sulfate reducing biofilm under dynamic conditions. A mathematical modeling approach for microbial growth and decay is proposed. Complete oxidizers sulfate reducing bacteria, incomplete oxidizers sulfate reducing bacteria and acetate degraders are the microbial groups taken into account in the model. The proposed model is able to simulate the competition among the bacteria growing in the biofilm. The method of characteristics is introduced for the numerical process. As in the qualitative analysis of solutions, where it was first presented, this method seems to be a powerful tool in this situation also. The model has been applied to simulate the sulfate reduction process in a biofilm for several purposes. In particular the effect of the COD/SO_4^{2-} ratio and the effect of different simulation times on the reactor performances in terms of volume fraction of bacterial species and substrate diffusion trends in biofilm have been assessed.

1. Introduction

Increasing anthropogenic activity has contributed to local imbalances in the natural sulfur cycle, leading to serious environmental problems. Industrial wastewater containing sulfate has contributed to this sulfur imbalance [1].

Sulfate can be removed from wastewaters by the chemical precipitation or desalination processes, but at high costs. Biological methods for the removal of sulfate from wastewater represent an attractive alternative.

A variety of reactors have been applied for the biological treatment of sulfate rich wastewater such as batch reactors [2], baffled reactors [3] and gas-lift reactors [4,5] that involve suspended-growth bacteria. Biological sulfate reducing processes that involve a bacterial biomass attached to media (biofilm), i.e. fixed bed reactors or fluidized bed reactors [6], have been developed in the last years. The environmental engineering processes that use a bacterial biomass attached to media have generally been referred to as fixed-growth processes.

Under anaerobic conditions dissimilatory sulfate reducing bacteria (SRB) use sulfate as a terminal electron acceptor for the degradation of organic compounds [7]. In this anaerobic process, sulfate is reduced to sulfide by the action of SRB which have the ability of coupling the oxidation of organic matter (electron donor) to the reduction of sulfate (electron acceptor) and depend on hydrolytic and fermentative bacteria that degrade complex organic matter [8].

The advantage of bacteria disposing in a biofilm is very important in an environmental industrial application. The bacteria in the biofilm, different from suspended bacteria, cannot be washed out with the water flow. This allows to retain the biomass within the reactor and therefore to operate at shorter hydraulic retention time (HRT). The bacterial biofilm allows to

* Corresponding author. Tel.: +39 0817683384.
E-mail addresses: dacunto@unina.it (B. D'Acunto), giovanni.esposito@unicas.it (G. Esposito), luigi.frunzo@unina.it (L. Frunzo), francesco.pirozzi@unina.it (F. Pirozzi).

0898-1221/$ – see front matter © 2011 Elsevier Ltd. All rights reserved.
doi:10.1016/j.camwa.2011.07.064

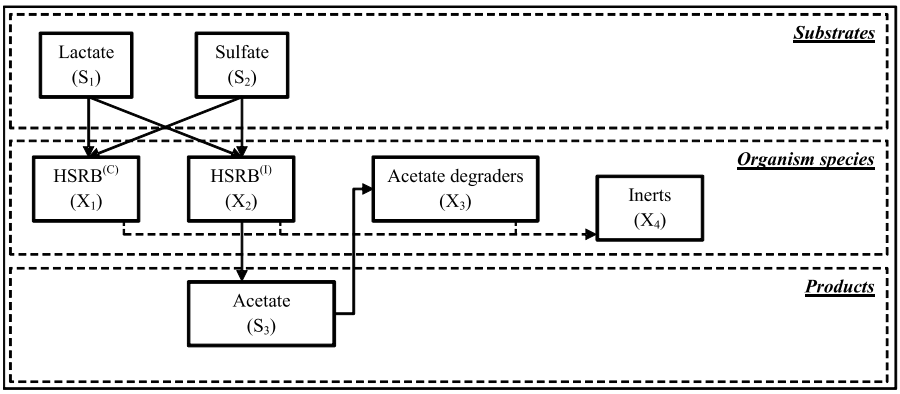

Fig. 2.1. Main pathways of a biological process.

achieve higher biomass concentration in bioreactors, and allows the growth of bacteria in bioreactor locations where their food remains abundant. Also, two main characteristics of biofilms offer great advantages in environmental applications: resistance to antimicrobial agents and formation of several bacterial species in biofilms. The resistance of antimicrobial agents allows a better resistance of bacteria when undesired inhibiting agents reach the wastewater treatment plant (shock loading). The formation of several bacterial species in biofilms allows to treat different organic and inorganic substrates at the same time. Biological sulfate reduction in anaerobic fixed growth reactors has been investigated extensively at lab-scale. In particular, it was pointed out that the composition of the microbial community influences the performance and stability of the overall biological sulfate reducing process [9]. Mathematical modeling of biofilms is usually based on continuum models, e.g. among others [10,11], and discrete-continuum models, e.g. [12]. As outlined in [13] the continuous approach can be related to the models at the macroscopic scale provided by methods of statistical mechanics. The model proposed in this work includes sulfate reduction by complete and incomplete sulfate reducing bacteria; COD removal by sulfate reduction and by acetogenic bacteria; acetate consumption via methanogenesis [9,14,15]. The biochemical mechanisms which regulate the competition between these trophic groups growing in anaerobic fixed growth reactors are nevertheless still mostly unknown. Thus, further research is needed to assess the effect of different process conditions on this competition and to define control criteria to favor the dominance of one species over the other. Mathematical models aimed at simulating the biochemical process prevailing in an anaerobic fixed growth reactor should be coupled to experimental studies in order to (i) address the laboratory experimental procedure; (ii) enhance the design and operation of the treatment systems [16]; and (iii) optimize the reactor process control criteria [5]. In this study a mathematical model was developed to describe the bacterial competition in sulfate reducing biofilms. The objectives of this study include:

- to propose a new mathematical modeling approach to study population dynamics competition between sulfate reducing and acetate degrading bacteria in biofilms;
- to propose a new numerical approach to solve a multispecies biofilm model;
- to describe substrate dynamics, i.e. mass transport of substrates and their microbial conversion, which take place within the biofilm.

2. Statement of the problem

We discuss the dynamics of a biological sulfate reducing biofilm. Physical, chemical and biological transient processes are analyzed. The kinetics of microbial growth and decay are modeled. The model considers the kinetics of three microbial species: complete oxidizers heterotrophic SRB (X_1), which completely oxidize lactate to CO_2, incomplete oxidizers heterotrophic SRB (X_2), which oxidize lactate to acetate, acetate degraders (X_3), and three reacting components (substrates and products): sulfate (S_1), lactate (S_2), acetate (S_3); see Fig. 2.1. The sulfate is used for the lactate oxidation by complete and incomplete SRB. Inert residues (X_4) are also taken into account.

The undesired formation of acetate allows the development of acetate degraders which compete for space in the biofilm with complete and incomplete heterotrophic SRB.

The biofilm growth is governed by the following equations [10,17],

$$\frac{\partial X_i}{\partial t} + \frac{\partial}{\partial z}(uX_i) = \rho_i r_{M,i}(z, t, \mathbf{X}, \mathbf{S}), \quad 0 \le z \le L(t),\ t > 0,\ i = 1, 2, 3, 4 \tag{2.1}$$

$$\frac{\partial u}{\partial z} = \sum_{i=1}^{4} r_{M,i}(z, t, \mathbf{X}, \mathbf{S}), \quad 0 < z \le L(t),\ t > 0, \tag{2.2}$$

where $X_i = \rho_i f_i(z, t)$ denotes the concentration of the microbial species and inert residues $i = 1, 2, 3, 4$, f_i denotes the volume fraction of microbial species i, $\sum_{i=1}^{4} f_i = 1$, ρ_i is the constant density, $u(z, t)$ is the velocity of the microbial

mass displacement with respect to the biofilm support interface, $S_j(z,t)$ is the concentration of the substrate $j = 1, 2, 3$, $r_{M,i}(z,t,X_i,S_j)$ is the biomass growth rate, $L(t)$ is the biofilm thickness, $\mathbf{X} = (X_1, X_2, X_3, X_4)$ and $\mathbf{S} = (S_1, S_2, S_3)$.

In addition, the biomass growth rates are given by

$$r_{M,1} = \mu_{\max,1} X_1 \frac{S_1}{K_{1,1}+S_1}\frac{S_2}{K_{2,1}+S_2} - b_{m,1}X_1, \tag{2.3}$$

$$r_{M,2} = \mu_{\max,2} X_2 \frac{S_1}{K_{1,2}+S_1}\frac{S_2}{K_{2,2}+S_2} - b_{m,2}X_2, \tag{2.4}$$

$$r_{M,3} = \mu_{\max,3} X_3 \frac{S_3}{K_{1,3}+S_3} - b_{m,3}X_3, \tag{2.5}$$

while for inert residues

$$r_{M,4} = b_{m,1}X_1 + b_{m,2}X_2 + b_{m,3}X_3, \tag{2.6}$$

where $\mu_{\max,i}$ denotes the maximum net growth rate for biomass i, $K_{i,j}$ is the half-saturation constant of substrate j for biomass i, $b_{m,i}$ is the decay-inactivation-rate concentration for biomass i.

The diffusion of substrates is governed by the equations

$$\frac{\partial S_j}{\partial t} - D_j \frac{\partial^2 S_j}{\partial z^2} = r_{S,j}(z,t,\mathbf{X},\mathbf{S}), \quad 0 < z < L(t),\ 0 < t \le T,\ j = 1,2,3, \tag{2.7}$$

where D_j denotes the diffusivity coefficient and $r_{S,j}(z,t,\mathbf{X},\mathbf{S})$ the conversion rate of substrate j. These are expressed by

$$r_{S,1} = -\frac{\mu_{\max,1}}{Y_1} X_1 \frac{S_1}{K_{1,1}+S_1}\frac{S_2}{K_{2,1}+S_2} - \frac{\mu_{\max,2}}{Y_2} X_2 \frac{S_1}{K_{1,2}+S_1}\frac{S_2}{K_{2,2}+S_2}, \tag{2.8}$$

$$\begin{aligned} r_{S,2} &= -1.5\frac{(1-Y_1)\mu_{\max,1}}{Y_1} X_1 \frac{S_1}{K_{1,1}+S_1}\frac{S_2}{K_{2,1}+S_2} \\ &\quad - 1.5\frac{(1-Y_2)\mu_{\max,2}}{Y_2} X_2 \frac{S_1}{K_{1,2}+S_1}\frac{S_2}{K_{2,2}+S_2}, \end{aligned} \tag{2.9}$$

$$r_{S,3} = \frac{(1-Y_2)\mu_{\max,2}}{Y_2} X_2 \frac{S_1}{K_{1,2}+S_1}\frac{S_2}{K_{2,2}+S_2} - \frac{\mu_{\max,3}}{Y_3} X_3 \frac{S_3}{K_3+S_3}, \tag{2.10}$$

where Y_i denotes the yield for biomass i.

The following initial-boundary conditions will be considered for Eqs. (2.1), (2.2) and (2.7)

$$X_i(z,0) = \varphi_i(z), \qquad u(0,t) = 0, \quad 0 \le z \le L_0,\ 0 < t \le T,\ i = 1,2,3,4, \tag{2.11}$$

$$S_j(z,0) = S_{j0}(z), \quad 0 \le z \le L_0,\ j = 1,2,3, \tag{2.12}$$

$$\frac{\partial S_j}{\partial z}(0,t) = 0, \qquad S_j(L(t),t) = S_{jL}(t), \quad 0 < t \le T,\ j = 1,2, \tag{2.13}$$

$$\frac{\partial S_3}{\partial z}(0,t) = \frac{\partial S_3}{\partial z}(L(t),t) = 0, \quad 0 < t \le T. \tag{2.14}$$

The functions $\varphi_i(z)$, $i = 1, \ldots, n$, represent the initial concentrations. Condition (2.11)$_2$ follows from the relationship $g_i(0,t) = u(0,t)X_i(0,t)$ of the biomass flux at $z = 0$. The functions $S_{j0}(z)$ represent the initial values of substrates. The functions $S_{jL}(t)$ in (2.13)$_2$ are the values of concentrations in the bulk liquid.

The free boundary evolution is governed by the following ordinary differential equation

$$\frac{\mathrm{d}L}{\mathrm{d}t}(t) = u(L(t),t), \tag{2.15}$$

with the initial condition

$$L(0) = L_0, \tag{2.16}$$

where L_0 denotes the initial biofilm thickness. Eq. (2.14) is derived from the general equation of the free boundary by setting the biomass flux $\sigma = 0$.

An existence and uniqueness theorem for the free boundary problem (2.1)–(2.15) was proved in [17] under quite general hypotheses. In addition, a number of properties for solutions was shown. Numerical methods will be discussed in the following section.

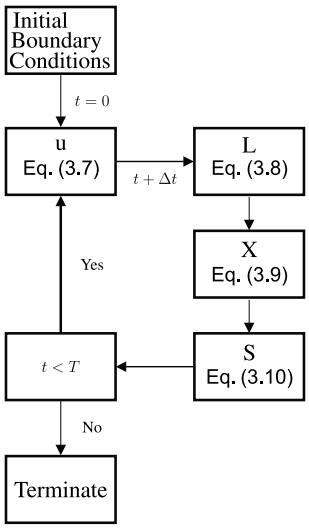

Fig. 3.1. Flow-chart.

3. Numerical methods

The qualitative analysis of system (2.1)–(2.15) developed in [17] was based on the method of characteristics. The success suggests that this method can be also used in the numerical analysis. In this section we show that the method can be applied very easily. In addition, it is less expensive than other methods and allows us to perform computational analysis of transient biofilm processes very efficiently.

The characteristics of system (2.1) are the lines $z = s(s^0, t)$ defined by

$$\dot{s}(s^0, t) = u(s(s^0, t), t), \qquad s(s^0, 0) = s^0, \quad 0 \le s^0 \le L_0, \ t > 0. \tag{3.1}$$

By introducing the characteristics and using the notations

$$G = \sum_i^4 r_{M,i} = G(z, t, \mathbf{X}, \mathbf{S}), \tag{3.2}$$

$$F_i = \rho_i r_{M,i} - X_i G = F_i(z, t, \mathbf{X}, \mathbf{S}), \tag{3.3}$$

system (2.1)–(2.2) is rewritten as

$$\frac{\partial u}{\partial s}(s, t) = G(s, t, \mathbf{X}, \mathbf{S}), \quad 0 < s \le L(t), \ t > 0, \tag{3.4}$$

$$\dot{X}_i(s(s^0, t), t) = F_i(s(s^0, t), t, \mathbf{X}, \mathbf{S}), \quad i = 1, 2, 3, 4, \ t > 0. \tag{3.5}$$

Consider Eq. (3.1). Integrating Eq. (3.1) over (t_n, t_{n+1}) yields

$$s_m^{n+1} - s_m^n = \int_{t_n}^{t_{n+1}} u(s(s_m^n, \tau), \tau) \mathrm{d}\tau, \tag{3.6}$$

where $s_m^n = s(s^m, t_n)$. Consider Eq. (3.4). Integrating over (s_m^n, s_{m+1}^n) yields

$$u(s_{m+1}^n, t_n) - u(s_m^n, t_n) = \int_{s_m^n}^{s_{m+1}^n} G(s, t_n, \mathbf{X}, \mathbf{S}) \, \mathrm{d}s. \tag{3.7}$$

Consider the free boundary equation (2.13). Integrating over (t_n, t_{n+1}) yields

$$L(t_{n+1}) - L(t_n) = \int_{t_n}^{t_{n+1}} u(L(\tau), \tau) \mathrm{d}\tau. \tag{3.8}$$

Furthermore, integrating Eq. (3.5) over (t_n, t_{n+1}) gives

$$X_i(s(s_m^n, t_{n+1}), t_{n+1}) - X_i(s(s_m^n, t_n), t_n) = \int_{t_n}^{t_{n+1}} F_i(s(s_m^n, \tau), \tau, \mathbf{X}, \mathbf{S}) \mathrm{d}\tau. \tag{3.9}$$

In Section 4, Eqs. (3.6)–(3.9) will be integrated by using a fourth-order Runge–Kutta method. The flow-chart is illustrated in Fig. 3.1.

Table 4.1
Operational parameters used for model simulations. Set 1.

Parameter	Unit	Set A	Set B	Set C	Set D
COD concentration	g COD l^{-1}	0.2	0.1	0.05	0.025
Sulfate concentration	g l^{-1}	0.2	0.2	0.2	0.2
Time simulation	h	12	12	12	12
Initial biofilm thickness	mm	2	2	2	2
Initial volume fraction of SRB	–	0.3	0.3	0.3	0.3
Initial volume fraction of SRB	–	0.3	0.3	0.3	0.3
Initial volume fraction of AD	–	0.3	0.3	0.3	0.3
Initial volume fraction of inert	–	0.1	0.1	0.1	0.1

Consider the diffusion equation (2.7). Finite difference methods for parabolic equations can be used, e.g. [18]. Recent finite difference methods introduced in [19,20] could also be experienced in future 2D and 3D applications. In Section 4, the forward Euler method will be used and we obtain

$$S_{j,m}^{n+1} = S_{j,m}^{n} + \frac{\Delta t}{(\Delta z)^2}(S_{j,m-1}^{n} - 2S_{j,m}^{n} + S_{j,m+1}^{n}) + \Delta \mathrm{tr}_{S,j,m}^{n}, \tag{3.10}$$

where

$$r_{S,j,m}^{n} = r_{S,j}(m\Delta z, n\Delta t, \mathbf{X}_m^n, \mathbf{S}_m^n). \tag{3.11}$$

4. Results and discussion

4.1. Simulation set 1: effect of the COD/SO_4^{2-} ratio on the biofilm sulfate removal performances

Parameter values used for the simulations

The mathematical model proposed in this paper has been applied to simulate the sulfate reduction process in a biological biofilm with an initial thickness of 2 mm. The initial conditions and biological parameters adopted in the simulations are reported in Table 4.1. Values of the kinetic parameters, stoichiometric parameters and mass transfer coefficients according to [5,21] were used except for the lactate mass transfer coefficient which resulted from the procedure proposed in [22].

By the application of empirical formula of [23], the molecular diffusion coefficient, earlier in water D_w and after in biofilm D_f, was determined. The formula can be described as follows:

$$D_w = 7.4 \times 10^{-8} \frac{(\varphi_b M_b)^{0.5} T}{\mu_b V_a^{0.6}}$$

where φ_b is the solvent association parameter (2.6 for water), M_b is the molecular weight of the solvent (18 g for water), T is the absolute temperature (expressed in K), μ_b is the solvent absolute viscosity (0.7208 cp for water at 35 °C), V_a are the molecular volumes of the solute as liquid at its normal boiling point (cm^3 mol^{-1}). To obtain the diffusion coefficients in the biofilm, the diffusion coefficients in water were multiplied by a factor of 0.8 to correct the additional diffusion resistance in the biofilm [24].

The computed values of molecular diffusion coefficients in dm^2 per *day* for sulfate, lactate and acetate are 0.00732 (dm^2/d), 0.00980 (dm^2/d) and 0.00835 (dm^2/d) respectively.

Figs. 4.1 and 4.2 show the results of model simulations performed to assess the COD/SO_4^{2-} ratio effect on the reactor performances in terms of volume fractions of bacteria and concentration trends of substrates in the biofilm for a 12 h simulation. COD/SO_4^{2-} ratios, in the range 0.125–1 were investigated.

Species and volumetric fractions of bacteria growing in the biofilm

First the influence of the COD/SO_4^{2-} ratio on the bacteria prevailing in the biofilm was studied. The simulated film structures at four different COD/SO_4^{2-} ratios are shown in Fig. 4.1. This figure indicates a high presence of acetate degraders at the inner layer of the biofilm whereas SRB are dominant over acetate degraders at the outmost layer of the biofilm. It is interesting to note that the area of acetate degraders in the biofilm becomes broader at decreasing COD/SO_4^{2-} ratios; see Fig. 4.1(C) and (D). This occurs since decreasing of COD surface load implies a lower sulfate reduction by the action of complete and incomplete SRB. In the deeper layers of the biofilm sulfate concentrations are lower than in the superficial layers of the biofilm, therefore the acetate degraders prevail over the SRB. When the COD/SO_4^{2-} ratio is low, the volumetric fraction of bacterial species is less homogeneous than at high COD/SO_4^{2-} ratios; see Fig. 4.1(C) and (D).

Trends of substrate concentrations in biofilm

The different kinds of bacterial species growing in the biofilm at different COD/SO_4^{2-} ratios imply a different concentration trend of substrates in the biofilm. Fig. 4.2 shows that a COD/SO_4^{2-} ratio increase causes an increase of sulfate reduction. When the COD/SO_4^{2-} ratio is 1, (see Fig. 4.2(A)) there is a sharp decrease of sulfate concentration throughout the biofilm

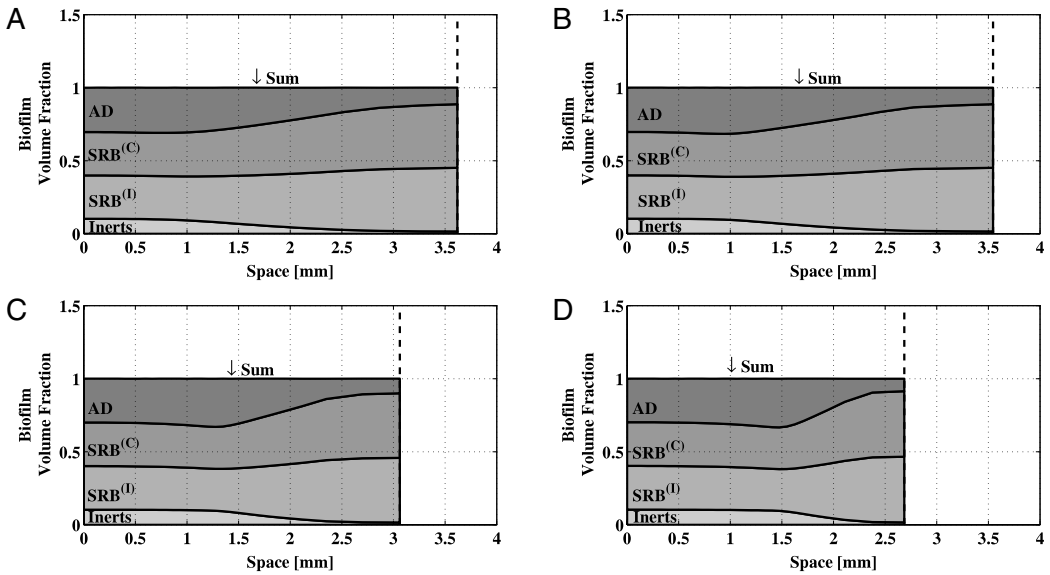

Fig. 4.1. Effect of the COD/SO_4^{2-} ratio on the volumetric fraction of the bacterial species in biofilm. A: $COD/SO_4^{2-} = 1$, B: $COD/SO_4^{2-} = 0.5$, C: $COD/SO_4^{2-} = 0.25$, D: $COD/SO_4^{2-} = 0.125$.

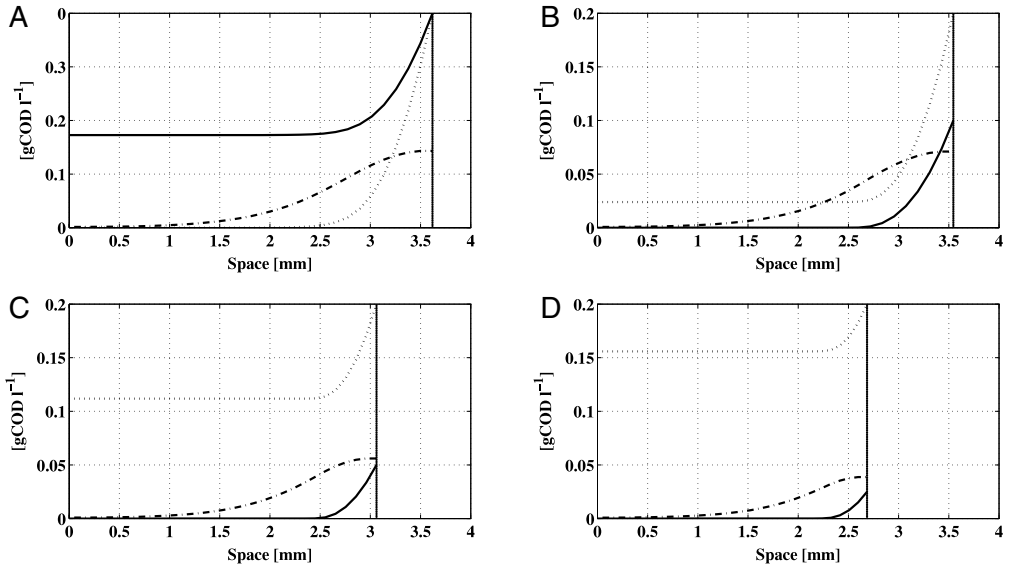

Fig. 4.2. Effect of the COD/SO_4^{2-} ratio on the substrate trends in biofilm. Dotted line: sulfate concentration; continuous line: COD concentration; dashdot line: acetate concentration. A: $COD/SO_4^{2-} = 1$, B: $COD/SO_4^{2-} = 0.5$, C: $COD/SO_4^{2-} = 0.25$, D: $COD/SO_4^{2-} = 0.125$.

depth, with a concentration near zero in the inner layer of the biofilm. This occurs because the concentration of COD is not limiting for SRB metabolism.

When the COD/SO_4^{2-} ratio is less than 0.5 (see Fig. 4.2(B)–(D)) COD is limiting implying a decrease in the sulfate reduction rate. Many authors have reported the accumulation of acetic acid in several types of reactors working under sulfate-reducing conditions, and most of them agree that acetate is the bottleneck of a sulfate reducing process [9]. It is interesting to note that the acetate production becomes broader at higher COD/SO_4^{2-} ratios. This was expected, since, at high COD/SO_4^{2-} ratios both complete and, in particular, incomplete SRB increase their metabolic activity, according to Eqs. (2.3) and (2.4).

The relationship between the COD/SO_4^{2-} ratio and the biofilm thickness is shown in Fig. 4.3. At high COD/SO_4^{2-} ratios there is no increase of the biofilm thickness. This is because SO_4^{2-} becomes a limiting substrate for biofilm bacteria metabolism and hence for the biofilm growth.

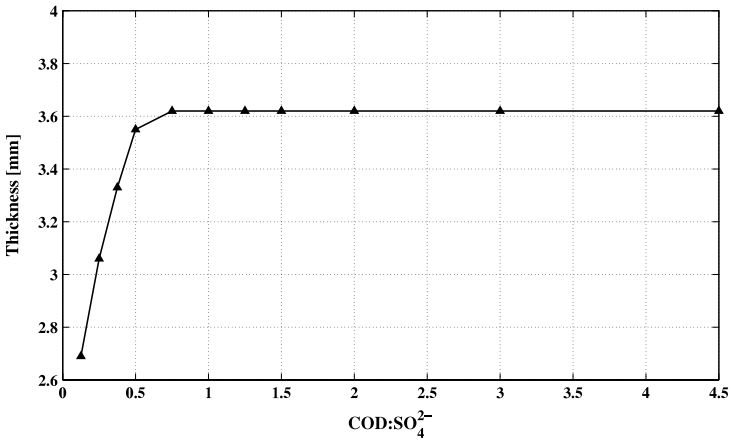

Fig. 4.3. Effect of the COD/SO_4^{2-} ratio on biofilm thickness.

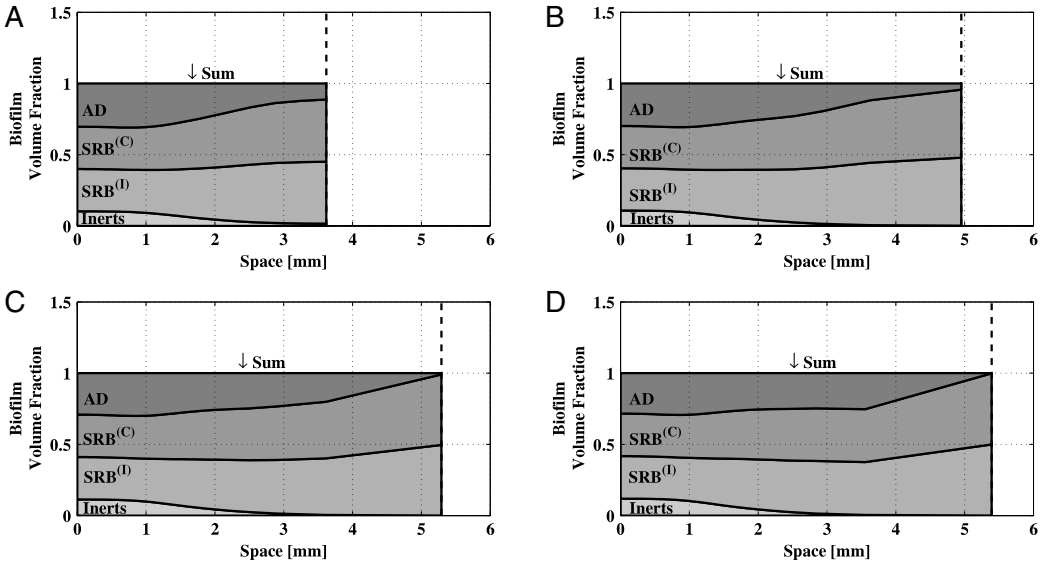

Fig. 4.4. Effect of simulation time on the volumetric fraction of the bacterial species in biofilm. A: Simulation time = 12 h, B: Simulation time = 24 h, C: Simulation time = 36 h, D: Simulation time = 48 h.

Table 4.2
Operational parameters used for model simulations. Set 2.

Parameter	Unit	Set A	Set B	Set C	Set D
COD concentration	g COD l^{-1}	0.2	0.2	0.2	0.2
Sulfate concentration	g l^{-1}	0.2	0.2	0.2	0.2
Simulation time	h	12	24	36	48
Initial biofilm thickness	mm	2	2	2	2
Initial volume fraction of SRB	–	0.3	0.3	0.3	0.3
Initial volume fraction of SRB	–	0.3	0.3	0.3	0.3
Initial volume fraction of AD	–	0.3	0.3	0.3	0.3
Initial volume fraction of inert	–	0.1	0.1	0.1	0.1

4.2. Simulation set 2: effect of simulation time on the biofilm sulfate removal performances

Species and volumetric fractions of bacteria growing in the biofilm

The effect of different simulation times was studied. When the simulation time increases the biofilm thickness increases, as expected. The effect of four different time simulations, and therefore, four different biofilm thicknesses are shown in Fig. 4.4. The initial conditions and biological parameters adopted in the simulations are reported in Table 4.2. Difference in the biofilm structure occurs when the time of simulation is greater than 1 day (see Fig. 4.4(C) and (D)). In this case AD are

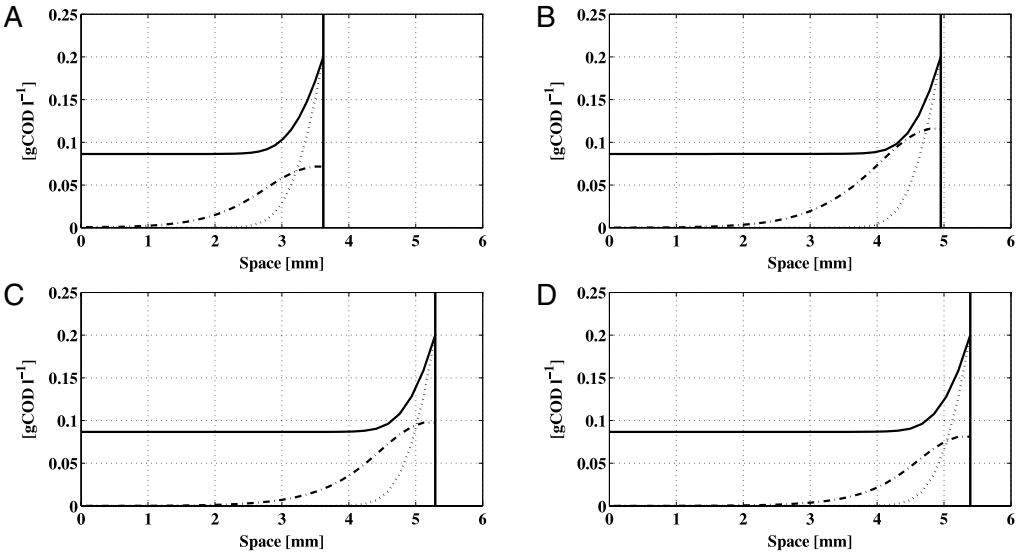

Fig. 4.5. Effect of simulation time on the substrate trends in biofilm. Dotted line: sulfate concentration; continuous line: COD concentration; dashdot line: acetate concentration. A: Simulation time = 12 h, B: Simulation time = 24 h, C: Simulation time = 36 h, D: Simulation time = 48 h.

predominantly active at the inner layer of the biofilm, while both complete and incomplete oxidizers SRB are found to be predominant at the outmost layer of the biofilm.

Trends of substrate concentrations in biofilm

The four different diffuse substrate concentration trends in the biofilm, for four different time simulations, are shown in Fig. 4.5. The trends of sulfate, COD and acetate concentrations are quite similar for the four simulations, which is in agreement with the Dirichlet boundary condition.

References

[1] P.N.L. Lens, A. Visser, A. Janssen, L.W. Hulstoff Pol, G. Lettinga, Biotechnological treatment of sulfate rich wastewaters, Crit. Rev. Environ. Sci. Technol. 28 (1) (1998) 41–88.
[2] L. Herrera, J. Hernandez, P. Ruiz, S. Gantenbein, Desulfovibrio desulfuricans growth kinetics, Environ. Toxicol. Water Qual. 6 (2) (1991) 225–237.
[3] A. Grobicki, D.C. Stuckey, Hydrodynamic characteristics of the anaerobic baffled reactor, Water Res. 26 (3) (1992) 371–378.
[4] G. Esposito, J. Wejma, F. Pirozzi, P.N.L. Lens, Effect of the sludge retention time on H_2 utilization in a sulfate reducing gas-lift reactor, Process Biochem. 39 (2003) 491–498.
[5] G. Esposito, P.N.L. Lens, F. Pirozzi, User-friendly mathematical model for the design of sulfate reducing H_2/CO_2 fed bioreactors, J. Environ. Eng. ASCE 135 (2009) 167–175.
[6] L.B. Celis-Garcia, G. Gonzalez-Blanco, M.J. Meraz, Chemical removal of sulfur inorganic compounds by a biofilm of sulfate reducing and sulfide oxidizing bacteria in a down-flow fluidized bed reactor, Technol. Biotechnol. 83 (3) (2008) 260–268.
[7] S.J.W.H. Oude Elferink, A. Visser, P.L.W. Hulshoff, A.J.M. Stams, Sulfate reduction in methanogenic bioreactors, FEMS Microbiol. Rev. 15 (2–3) (1994) 119–136.
[8] F. Widdel, Microbiology and ecology of sulfate and sulphur reducing bacteria, in: A.J.B. Zehnder (Ed.), Biology of Anaerobic Microorganisms, John Wiley & Sons, New York, 1988.
[9] L.B. Celis, D. Villa-Gomez, A.G. Alpuche Solis, B.O. Ortega Morales, E. Razo Flores, Characterization of sulfate-reducing bacteria dominated surface communities during start-up of a down-flow fluidized bed reactor, J. Ind. Microbiol. Biotechnol. 36 (1) (2008) 111–121.
[10] O. Wanner, W. Gujer, A multispecies biofilm model, Biotechnol. Bioeng. 28 (1986) 314–328.
[11] I. Klapper, J. Dockery, Mathematical description of microbial biofilms, SIAM Rev. 52 (2010) 222–265.
[12] E. Alpkwist, C. Picioreanu, M.C.M. Van Loosdrecht, A. Heyden, Three-dimensional biofilm model with individual cells and continuum EPS matrix, Biotechnol. Bioeng. 94 (5) (2006) 961–979.
[13] N. Bellomo, A. Bellouquid, J. Nieto, J. Soler, Multiscale biological tissue models and flux-limited chemotaxis from binary mixtures of multicellular growing systems, Math. Models Methods Appl. Sci. 20 (2010) 1179–1207.
[14] M. Gallegos-Garcia, L.B. Celis, R. Rangel-Méndez, E. Razo Flores, Precipitation and recovery of metal sulfides from metal containing acidic wastewater in a sulfidogenic down-flow fluidized bed reactor, Biotechnol. Bioeng. 102 (1) (2009) 91–99.
[15] D.J. Batstone, J. Keller, I. Angelidaki, S.V. Kalyuzhnyi, S.V. Pavlostathis, A. Rozzi, W.T.M. Sanders, H. Siegrist, V.A. Vavilin, Anaerobic Digestion Model No. 1, Scientific and Technical Report No. 13, IWA Publishing, 2002.
[16] M. Henze, W. Gujer, M.T. Van Loosdrecht, Activated Sludge Models ASM1, ASM2, ASM2d and ASM3, Scientific and Technical Report No. 9, IWA Publishing, 2000.
[17] B. D'Acunto, L. Frunzo, Qualitative analysis and simulations of a free boundary problem for multispecies biofilm models, Math. Comput. Modelling 53 (2011) 1596–1606.
[18] B. D'Acunto, Computational Methods for PDE in Mechanics, World Scientific, Singapore, 2004.
[19] F. Brezzi, K. Lipnikov, M. Shashkov, Convegergence of mimetic finite difference method for diffusion problems on polyhedral meshes with curved faces, Math. Models Methods Appl. Sci. 16 (2) (2006) 275–297.
[20] K. Lipnikov, G. Manzini, F. Brezzi, A. Buffa, The mimetic finite difference methodfor the 3D magnetostatic field problems on polyhedral meshes, J. Comput. Phys. 230 (2) (2011) 305–328.
[21] P.S. Stewart, Diffusion in biofilms, J. Bacteriol. (2003) 1485–1491.
[22] H. Lin Yen, K. Lee Kwang, Verification of anaerobic biofilm model for phenol degradation with sulfate reduction, J. Environ. Eng. 127 (2) (2001) 119–125.
[23] C.E. Wilke, P. Chang, Correlation of diffusion coefficients in dilute solutions, AIChE J. 1 (1955) 264–270.
[24] K. Williamson, P.L. McCarty, Verification studies of the biofilm model for bacterial substrate utilization, J. Water Pollut. Control Fed. 48 (1976) 281–296.